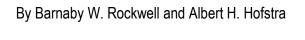


Mapping Argillic and Advanced Argillic Alteration in Volcanic Rocks, Quartzites, and Quartz Arenites in the Western Richfield 1° x 2° Quadrangle, Southwestern Utah, Using ASTER Satellite Data



Open-File Report 2012-1105

U.S. Department of the Interior U.S. Geological Survey

U.S. Department of the Interior

Ken Salazar, Secretary

U.S. Geological Survey

Marcia K. McNutt, Director

U.S. Geological Survey, Reston, Virginia: 2012

For product and ordering information:

World Wide Web: http://www.usgs.gov/pubprod

Telephone: 1-888-ASK-USGS

For more information on the USGS—the Federal source for science about the Earth, its natural and living resources, natural hazards, and the environment:

World Wide Web: http://www.usgs.gov Telephone: 1-888-ASK-USGS

Any use of trade, product, or firm names is for descriptive purposes only and does not imply endorsement by the U.S. Government.

Although this report is in the public domain, permission must be secured from the individual copyright owners to reproduce any copyrighted material contained within this report.

Suggested citation:

Rockwell, B.W., and Hofstra, A.H., 2012, Mapping argillic and advanced argillic alteration in volcanic rocks, quartzites, and quartz arenites in the western Richfield 1° x 2° quadrangle, southwestern Utah, using ASTER Satellite Data: U.S. Geological Survey Open-File Report 2012–1105, 5 p., 1 plate.

Contents

ntroductionntroduction	٠
ASTER Data and Reflectance Calibration	
Mineral Mapping Results	
Conclusions	
References Cited	

Mapping Argillic and Advanced Argillic Alteration in Volcanic Rocks, Quartzites, and Quartz Arenites in the Western Richfield 1° x 2° Quadrangle, Southwestern Utah, Using ASTER Satellite Data

By Barnaby W. Rockwell and Albert H. Hofstra

Introduction

Rockwell and Hofstra (2009a) published preliminary results of a mineral mapping survey in southwestern Utah derived from spectroscopic analysis of digital imagery acquired by the Advanced Spaceborne Thermal Emission and Reflection Radiometer (ASTER) sensor. This report provides a poster with updated mapping results of clay-sulfate-mica-carbonate minerals and added ferric iron occurrence in printable and zoomable Portable Document Format (PDF). Two versions of the poster are provided that vary in file size and image quality related to the type of JPEG2000 compression. The version with the smaller file size (71.4 MB) was produced with maximum quality compression, and is designed for faster download, viewing, and printing. The version with the larger file size (239 MB) was produced with lossless compression and is optimal for detailed, zoomed viewing, and high-quality printing.

The poster compares mineral maps generated from analysis of combined visible-near infrared (VNIR) and shortwave-infrared (SWIR) data (updated for this report) and thermal infrared (TIR) data to a previously published regional geologic map. Such comparisons are used to identify rock-forming and hydrothermal alteration-related minerals to aid in lithologic mapping and alteration characterization over an area 11,245 square kilometers in size.

Digital maps in geospatial PDF format are also provided that show the ASTER-derived interpretive data from the poster. These maps are designed for field work on portable computers. The geographic coordinates of any location in the maps will be displayed at the lower right of the Acrobat Reader window. Sheet 1 shows the mineral mapping derived from analysis of the ASTER VNIR and SWIR data (central poster frame). Sheet 2 shows the quartz and carbonate mapping derived from analysis of TIR data (right-hand poster frame).

ASTER Data and Reflectance Calibration

Four overlapping ASTER scenes from 2000 and 2004 were used for mapping clay, sulfate, mica, carbonate, sorosilicate, and hydrous silica minerals using the VNIR and SWIR regions of the electromagnetic spectrum. These scenes were acquired in two parallel paths. The two scenes from the western path were acquired on August 27, 2004, and the two scenes from the eastern path were acquired on July 31, 2000.

To prepare the ASTER data for quantitative analytical comparison to reference laboratory spectra, the data were calibrated to reflectance format using laboratory spectra of a field calibration site. Crosstalk-related errors in the SWIR data were mitigated by subtracting non-zero minimum values from each SWIR band (Rockwell, 2009). SWIR band minima were computed separately for the two scene acquisition dates. The ASTER bands were then converted to radiance units through multiplication by scene-specific gain values. A high-resolution spectrum of smectite-bearing alluvium from Wah Wah Wash in the central Wah Wah Valley was measured in the laboratory. This spectrum was divided by an average ASTER radiance spectrum of the field calibration site from the 2000 data, producing a correction spectrum that was multiplied by the ASTER 2000 radiance image data to generate 9-band datasets in reflectance format (Rockwell and others, 2002).

To calibrate the 2004 ASTER data to reflectance, a bootstrap procedure was performed (Rockwell and others, 1999) that used the calibrated 2000 data as a reference reflectance base. An average spectrum of a site covered by both the 2000 and 2004 data was sampled from the 2000 reflectance data. This spectrum was divided by an average spectrum of the same site sampled from the 2004 radiance data, generating a correction spectrum. This correction spectrum was multiplied by the 2004 radiance data, generating 9-band datasets in reflectance format.

ASTER thermal infrared (TIR) surface emissivity data of the 2004 scenes and a scene from April 23, 2002, were used to map quartz and carbonate minerals using techniques described by Rockwell and Hofstra (2008).

All ASTER data were orthorectified using a Projective Transform to mosaicked TerraServer digital orthophoto quadrangles, digital raster graphics, and a 1/3-arc-second digital elevation model (~10 m resolution) from the USGS National Elevation Dataset (NED, provided by USGS Seamless Data Distribution System).

Mineral Mapping Results

The mineral identifications generated from spectroscopic analysis of combined VNIR-SWIR data (Rockwell, 2009) from the four ASTER scenes shown in the central panel are overlain on top of one another, and not mosaicked using cutlines to eliminate scene overlap. Mineral identifications from multiple scenes will thus be shown in the overlap areas of the scenes. TIR data analysis results shown in the right-hand panel have been mosaicked.

Occurrences of ferric iron-bearing minerals (for example, hematite, goethite, and jarosite) in high abundance identified from the ASTER VNIR-SWIR data are overlain as hollow, black polygons on the other mineral mapping results of the central panel. The ferric iron results have been simplified using a 3 x 3 majority filter to remove single-pixel occurrences. Ferric iron in lower abundance has been removed for simplicity, and occurs widely on alluvial surfaces.

Mineral identifications in areas of corrupted SWIR data related to the detector "scratch" can be erroneous, and are described by Rockwell (2009 and references therein). There are two parallel strips of partially corrupted data in every scene, and thus four strips in the study area from the 2000 and 2004 ASTER data. These areas are indicated in the central map on the poster. Identifications of kaolinite- or alunite-bearing assemblages (ASTER band 5 absorptions) may be erroneous within the western strip from each acquisition date, and jarosite, dolomite, and hydrous silica (ASTER band 7 absorptions) may be erroneous within the eastern strip.

Intense quartz-sericite alteration hosted by the Horn Silver Andesite was mapped in the Beaver Lake Mountains northwest of Milford. Clay-rich zones of quartz, kaolinite and (or)

smectite +/- ferric iron were identified within this altered area, and may indicate more pyritic zones of phyllic alteration having a supergene argillic overprint. The small occurrences of ferric iron in these zones, which show excellent spatial correlation with high-abundance quartz identified using the TIR data, are not shown on the central panel because they were removed by the majority filtering process. Quartz, sericite, and ferric iron were mapped in disturbed ground associated with an open-pit mining operation on the south-central flank of the range within a propylitically-altered Tertiary intrusion (Ti on geologic map). The mineral mapping has not been field verified in this area.

Quartzites are well-mapped using the TIR data, and are shown on the right-hand panel in red colors along with quartz-rich sand deposits. Unaltered quartzites typically contain abundant sericite with little to no clay content (central panel).

This study detected previously unknown, quartzite-hosted advanced argillic alteration in the San Francisco Mountains produced by hydrothermal fluids that may be derived from unmapped calc-alkaline intrusions or unexposed cupolas north of the Preuss and Newhouse mining districts.

Fracture- and bedding plane-controlled advanced argillic alteration within older quartzite units was mapped in a 12-km-diameter halo surrounding the Pine Grove porphyry molybdenum deposits (Rockwell and Hofstra, 2009b). Pyrophyllite identified using the ASTER data in quartzite 3.5 km west of the Pine Grove deposit has been verified in the laboratory.

Pixels with spectra similar to that of pyrophyllite were identified within the central parts of thick alunite deposits in the NG Alunite area south of Pine Grove. Pyrophyllite has not been confirmed in that area, and these pixels likely represent very abundant and pure (clay-free) alunite. Alunite and pyrophyllite are difficult to reliably distinguish from each other using ASTER data (Rockwell, 2009).

At Wah Wah Summit, a previously unknown exposure of mixed Na-K alunite, kaolinite, and high-aluminum sericite was detected adjacent to a Tertiary calc-alkaline intrusion.

Quartz-alunite alteration identified within younger, rhyolitic volcanic rocks (Steamboat Mountain Formation, 13–12 Ma) of the Broken Ridge area (including Mountain Spring Peak) and Bible Springs fault zone correlate well with such alteration mapped by Duttweiler and Griffitts (1989). Quartz content of this alteration is highly variable and locally significantly greater than in alunite-bearing alteration of the NG Alunite area and Shauntie Hills (22.5–20.6 Ma) to the north. The quartz is primarily non-hydrous, and may occur without alunite. The most abundant hydrothermal quartz (colored red in right-hand poster panel) is associated with alunite, either intimately or in close proximity.

Excellent spatial correlation exists between carbonate rocks shown on the geologic map, calcite and dolomite identified from the SWIR data analysis, and carbonate rocks identified from the TIR data analysis. The spectroscopic analysis of the SWIR data using least-squares curve fitting techniques to match image spectra with reference laboratory spectra (Rockwell, 2009 and references therein) is more sensitive to low-abundance carbonate in alluvium than the ratio-based analysis of the TIR data.

Scattered pixels in the Broken Ridge area, southern Wah Wah Mountains, and southern Indian Peak Range, were identified as dolomite (colored dark green on map in center panel). Many of these pixels occur in volcanic rocks covered with dense growth of piñon pine, juniper, and grasses. The grasses have senesced by the mid to late summer data acquisition dates, revealing SWIR absorption features related to leaf biochemicals such as lignin and cellulose. Pixels in these areas have weak or absent absorptions at ASTER bands 2 and 7 and deeper

absorption at bands 7–8 with a spectral shape matching that of dolomite. Although all ASTER pixels are screened for green (chlorophyll absorption at ASTER band 2) and dry (lignin-cellulose absorption at bands 7 and 8–9) vegetation (Rockwell, 2009), these pixels passed through the screening and are a spectral match to dolomite in low abundance (shallow feature depth). Although soils in these areas may contain caliche, which will provide a carbonate spectral response, many of the dolomite detections in these areas are most likely erroneous and represent spectral confusion with dry vegetation.

Conclusions

This report demonstrates that spectroscopic analysis of ASTER multispectral VNIR-SWIR data, especially when coupled with ratio-based analysis of ASTER TIR data, is highly effective for mapping mineralogy associated with unaltered, metamorphosed, and hydrothermally-altered rocks. The mapping was critical in locating previously unrecognized exposures of advanced argillic alteration including those hosted by quartzites surrounding the Pine Grove porphyry molybdenum deposit and the Preuss and Newhouse polymetallic mining districts in the San Francisco Mountains. ASTER data analysis is capable of identifying quartzites by their high quartz content, and of differentiating clay-bearing, altered quartzites from unaltered quartzites that typically contain only sericite of primary detrital and (or) authigenic origin in the groundmass. Massive carbonate units can be mapped using the TIR data, and the SWIR data can be used to map carbonate in lower abundance, including on alluvial surfaces, and to differentiate calcite from dolomite. This report also demonstrates that results of detailed spectroscopic analysis of ASTER VNIR-SWIR data are consistent between multitemporal ASTER scenes and can thus be combined into virtually seamless, regional mineral maps.

References Cited

- Duttweiler, K.A., and Griffitts, W.R., 1989, Geology and geochemistry of the Broken Ridge area, southern Wah Wah Mountains, Iron County, Utah: U.S. Geological Survey Bulletin, Report: B 1843, 32 pp., 1 sheet.
- Rockwell, B.W., 2009, Comparison of ASTER- and AVIRIS-derived mineral and vegetation maps of the White Horse replacement alunite deposit and surrounding area, Marysvale volcanic field, Utah: U.S. Geological Survey Scientific Investigations Report 2009–5117, 31 p. (Also available at http://pubs.usgs.gov/sir/2009/5117/.)
- Rockwell, B.W., Clark, R.N., Livo, K.E., McDougal, R.R., and Kokaly, R.F., 2002, AVIRIS Data Calibration Information: Oquirrh and East Tintic Mountains, Utah: U.S. Geological Survey Open-File Report 02–0200, http://pubs.usgs.gov/of/2002/ofr-02-0200/.
- Rockwell, B.W., Clark, R.N., Livo, K.E., McDougal, R.R., Kokaly, R.F., and Vance, J.S., 1999, Preliminary materials mapping in the Park City region for the Utah USGS-EPA Imaging Spectroscopy Project using both high- and low-altitude AVIRIS data: 8th Annual JPL Airborne Earth Science Workshop, R.O. Green, ed., NASA JPL Publication 99–17, Pasadena, California, USA, February, 1999. (HTML version available at http://speclab.cr.usgs.gov/earth.studies/Utah-Upark.cityAV5.html; PDF file available at
 - http://speclab.cr.usgs.gov/earth.studies/Utah-1/park_cityAV5.html; PDF file available at ftp://popo.jpl.nasa.gov/pub/docs/workshops/99 docs/51.pdf.)
- Rockwell, B.W., and Hofstra, A.H., 2008, Identification of quartz and carbonate minerals across northern Nevada using ASTER thermal infrared emissivity data—Implications for geologic

- mapping and mineral resource investigations in well-studied and frontier areas: Geosphere, v. 4, no. 1, p. 218–246, doi: 10.1130/GES00126.1.
- Rockwell, B.W. and Hofstra, A.H., 2009a, Mapping argillic and advanced argillic alteration in volcanic rocks, quartzites, and quartz arenites in the western Richfield 1° x 2° quadrangle, southwestern Utah, using ASTER satellite data (abstract): Geological Society of America Rocky Mountain Section Meeting Abstracts with Programs, Orem, Utah, May 11–13, 2009, v. 41, no. 6, p. 39. (Also available at
 - http://gsa.confex.com/gsa/2009RM/finalprogram/abstract 157802.htm.)
- Rockwell, B.W., and Hofstra, A.H., 2009b, Remote detection of argillic alteration in quartzites and quartz arenites above and distal to porphyry Cu and Mo deposits: implications for assessments of concealed deposits: Geological Society of America Rocky Mountain Section Meeting Abstracts with Programs, Orem, Utah, May 11–13, 2009, v. 41, no. 6, p. 6. (Also available at http://gsa.confex.com/gsa/2009RM/finalprogram/abstract_157797.htm.)